Journal of Marine Systems 128 (2013) 40–51

Contents lists available at ScienceDirect

Journal of Marine Systems

journal homepage: www.elsevier.com/locate/jmarsys

Controls on riverine $\delta^{30}Si$ signatures in a temperate watershed under high anthropogenic pressure (Scheldt — Belgium)

C. Delvaux [a,*,1], D. Cardinal [a,1,2], V. Carbonnel [b,3], L. Chou [b], H.J. Hughes [a], L. André [a]

[a] Department of Geology and Mineralogy, Royal Museum for Central Africa, Tervuren, Belgium
[b] Service de Biogéochimie et Modélisation du Système Terre, Océanographie Chimique et Géochimie des Eaux, Département des Sciences de la Terre et de l'Environnement, Université Libre de Bruxelles, Brussels, Belgium

ARTICLE INFO

Article history:
Received 25 January 2012
Received in revised form 10 January 2013
Accepted 23 January 2013
Available online 31 January 2013

Keywords:
Silicon isotopes
Catchment
Season
Land-use
Tributaries
Silicon continental cycle
Scheldt

ABSTRACT

We analysed Si isotopic signatures ($\delta^{30}Si$ signature) of dissolved silicon (DSi) in the Scheldt (Belgium) tidal river (four stations) and in its main tributaries (Zenne, Dender, Grote Nete and Kleine Nete). For each station, we analysed four samples representative of the four seasons. These are the first $\delta^{30}Si$ data at the basin and seasonal scales measured in a watershed under high anthropogenic pressure. In the Scheldt main stem, we show that the role of diatoms on the silicon biogeochemical cycle and $\delta^{30}Si$ signatures is dominant in summer and sometimes in fall. Out of the diatoms' growing season, the Scheldt main stem exhibits unexpected large $\delta^{30}Si$ signatures variations, especially in winter. Although these isotopic variations are not reflected in DSi concentrations, they are consistent with $\delta^{30}Si$ signatures recorded in the main tributaries. This indicates that except for summer diatom blooms, $\delta^{30}Si$ signatures in the tidal river result from a conservative mixing with tributaries. Overall we suggest that the variations are mainly set by land use and lithology at the sub-basin level. Forest cover (inducing clay dissolution favoured by the presence of humic acids) and wetland cover (yielding to dissolution of biogenic silica) are highly and significantly correlated with $\delta^{30}Si$ ($R^2 > 0.85$). Both environments tend to render the tributaries $\delta^{30}Si$ signatures lighter while agriculture cover has the reverse effect on $\delta^{30}Si$ values ($R^2 = 0.70$, p-value < 0.08). In contrast, urban zone cover does not have any noticeable effect on Si isotopic signatures of the Scheldt tributaries. Despite this effect of land use, we estimate a mean annual $\delta^{30}Si$ signature output from the Scheldt tidal river to the saline estuary at 0.95‰, well comparable to other rivers. This results from the mixing of tributaries within the tidal river which levels off at the outlet the Si isotopic differences of the sub-basins. In the Scheldt watershed, it thus seems that Si isotopes could trace anthropogenic activities at the sub-basin scale. In contrast, at the outlet, the variety of land-use and lithology found over the whole watershed are merged into a mean isotopic signature similar to the world river average. As it is now recognised that change in land use alter the silicon biogeochemical continental cycle, our data show that use of Si isotopic signatures might constitute a useful proxy to better trace these modifications on contrasted (sub-)basins.

1. Introduction

Silicon (Si) is the second most abundant element of the Earth's upper crust. In aquatic ecosystems, most of the dissolved silicon, principally present as silicic acid (H_4SiO_4 hereafter referred to as DSi), is originally produced during weathering of silicate minerals on land, which is a slow process compared to biological time-scales (Canfield et al., 2005). In the terrestrial cycle, higher plants take up DSi through their roots and deposit it in their leaves and stem as opal particles (amorphous hydrated biogenic SiO_2, hereafter referred to as BSi) called phytoliths (Conley, 2002). DSi may be beneficial for the development of plants, their yield, their resistance to external stresses and their defence against fungal and insect attack (e.g. Belanger et al., 2003; Epstein, 1999; Reynolds et al., 2009). However, since BSi is more soluble than lithogenic Si present in crystalline minerals, such soil–plant cycle also contributes to the release of DSi in rivers (e.g. Alexandre et al., 1997; Conley, 2002; Cornelis, 2010; Derry et al., 2005; Meunier et al., 2010). For the aquatic ecosystem, DSi is an essential nutrient for the growth of diatoms, a key phytoplankton group in rivers and coastal zones (Martin-Jézéquel et al., 2000; Ragueneau et al., 2000, 2006).

Due to the specific need for silicon by diatoms, the availability of DSi and its relative abundance compared to other nutrients (e.g. nitrates and phosphates) can influence the composition of the phytoplankton

* Corresponding author at: Department of Geology and Mineralogy, Royal Museum for Central Africa, 3080 Tervuren, Belgium. Tel.: +32 2 769 54 56.
E-mail address: claire.delvaux@africamuseum.be (C. Delvaux).
[1] These two authors have equally contributed to this work and are co-lead authors.
[2] Now at: Laboratoire d'Océanographie et du Climat: Expérimentations et Approches Numériques, Université Pierre & Marie Curie, Paris, France.
[3] Now at: Geography Department, Peking University, Yiheyuan Road, Haidian District, Beijing 100871, PR China.

0924-7963/$ – see front matter © 2013 Elsevier B.V. All rights reserved.
http://dx.doi.org/10.1016/j.jmarsys.2013.01.004

community. In many ecosystems, human perturbation has resulted in an excess load of nitrogen (N) and phosphorus (P) compared to Si. This surplus of N and P allows the development of blooms of non-siliceous algae after the spring diatom bloom. Higher trophic levels and the functioning of the entire ecosystem may then be altered (Conley et al., 1993; Lancelot, 1995; Officer and Ryther, 1980; Turner et al., 1998).

The ubiquity of silicon at the Earth's surface and its chemical specificity (e.g. its difficulty to solubilise and isolate during sample processing in the laboratory) make the tracking of its biogeochemical cycling challenging. However, the fractionation of stable Si isotopes provides crucial information for a better understanding of chemical and biological processes in both terrestrial and marine environments (e.g. De la Rocha et al., 2000; Ziegler et al., 2005). Recent studies have shown that Si isotopic compositions of DSi in rivers can exhibit significant seasonal variation with δ^{30}Si ranging generally from +0.6‰ to +1.2‰ (Engström et al., 2010; Georg et al., 2006; Hughes et al., 2011). However, only two studies were carried out in a temperate region (Ding et al., 2004; Georg et al., 2006) and the one of Ding et al. (2004) report values up to +3.4‰. The Si isotopic signatures of DSi may also reflect biological, anthropogenic and geochemical characteristics at sub-basin scale. Few studies examined, directly or indirectly, this last aspect in rivers and tributaries (Cardinal et al., 2010; Engström et al., 2010; Hughes et al., under revision).

The Scheldt watershed has a total drainage area of approximately 19,900 km^2 spreading over northern France, Belgium and The Netherlands where it discharges into the North Sea (Passy et al., 2013–this volume). Within this densely populated area (>500 inhabitants per km^2), the landscape has been deeply affected for centuries by agriculture and active industrial development. Changes in land use and, more recently, increased inputs of fertiliser resulted in a marked lowering of DSi export (Struyf et al., 2010). Intensive agriculture and animal farming have also led to eutrophication impacting the ecological functioning of the Scheldt watershed (Cox et al., 2009). Although there is an unmistakable link between intensive agricultural activity and the occurrence of high nutrient concentrations in the aquatic environment, few data are available regarding the contribution of agricultural activity to the total nutrient loads (Vandenberghe et al., 2005). The Si-cycle in the Scheldt is highly affected by anthropic activities, although mainly in an indirect and diffuse way. Direct anthropogenic pressures (e.g., detergents, paper production processes, and sewage inputs) are probably limited as shown by Sferratore et al. (2006) for the Seine watershed. We measured in this paper the seasonal variations of the δ^{30}Si signatures in the eutrophied Scheldt tidal river and its five main tributaries in order to investigate how these signatures are affected by human pressure such as land use.

2. Material and methods

2.1. Study area

The Scheldt River includes an estuary with a salinity gradient (downstream Hemiksem) and an upstream freshwater part still under the tidal influence (hereafter called "tidal river", stretching from Ghent to Hemiksem) (Fig. 1). The Scheldt tidal river (annual average discharge at tidal limit, i.e. Ghent, in 2003: 37.2 m^3/s) directly receives water from the Dender (11.1 m^3/s) on the western part and, on the eastern part, from the Zenne (9.1 m^3/s), the Dijle (28.3 m^3/s), the Grote Nete (7.3 m^3/s) and the Kleine Nete (9.4 m^3/s) via the Nete and the Rupel (Fig. 1). The tidal wave is artificially blocked by sluices at Ghent and at the mouth of the Dender, but decreases naturally in the tributaries of the Rupel. The Durme is a closed river and its discharge is negligible. Our investigation focuses on the tidal river and its major tributaries.

The land-use over the Scheldt watershed (including tributaries) is dominated by agricultural activities (from 34 to 63%): arable land (only crop, legume, etc.) and heterogeneous agricultural area (mosaic of annual crop, grazing land, natural area, and woody cover). The area occupied by urban zone is ranging from 23 to 40%. A significant woody cover is only present in Kleine Nete and Grote Nete (21 and 17% respectively) (Corine Land Cover 2006).

2.2. Sampling

The Scheldt tidal river (from Ghent to Hemiksem) and the five main tributaries (Dender, Zenne, Dijle, Grote Nete, and Kleine Nete) were monitored weekly for DSi and BSi concentrations during 2003 (Carbonnel et al., 2009). The tidal river was sampled at four stations (Fig. 1): Ghent (157 km from the mouth, limit of the tidal influence), Dendermonde (124 km from the mouth), Temse (101 km from the mouth) and Hemiksem (91 km from the mouth). The tributaries of the Rupel were sampled at the limits of the tidal influence (Fig. 1). Among these samples, we selected three periods, each characteristic of one particular season: winter (17–18th March, before spring bloom), spring (26–27th May) and fall (27th October). Details of the sampling procedure and storage are given in Carbonnel et al. (2009). Briefly, from 20 to 150 ml of river water were collected at all sampling stations and vacuum filtered through 0.45 μm pore size polycarbonate membranes within 24 h. The filtrate was acidified and stored in polypropylene tubes at 4 °C in the dark. Because not enough solution was left from the 2003 summer sampling, a new field campaign was performed in summer 2008 (8th August) and samples were processed as described previously. In Section 4.3.2 we discuss the comparability of these two summers. For the 2003 sampling, DSi and BSi are available from Carbonnel et al. (2009) where the methods are detailed. Briefly DSi was measured colorimetrically on a Skalar Auto-analyser following a method adapted from Koroleff (1983). BSi was first extracted using a wet alkaline method (Carbonnel et al., 2009) and then the concentrations in the leaches were determined for Si by colorimetry on a Skalar Auto-analyser (as for DSi) and for Al following Dougan and Wilson (1974). For the summer 2008 sampling, DSi was analysed by colorimetry (Koroleff, 1983).

2.3. Isotopic analyses

To avoid any isotopic bias due to matrix effect, DSi purification prior to isotopic analyses was achieved through a quantitative reaction with triethylamine-molybdate (TEA-moly) coprecipitation and combustion in covered Pt crucibles at 1000 °C (De La Rocha et al., 1996). The solid residue was dissolved in diluted Suprapur HCl-HF at 90 °C (Cardinal et al., 2003). Silicon, molybdenum and major elements were then measured by ICP-AES to control Si recovery and to confirm that no other contaminant remained in purified Si solutions (Cardinal et al., 2003). During the transfer of cristoballite from Pt crucibles to dissolution beakers, some mechanical loss can occur but such loss cannot bias the δ^{30}Si signature of the sample. Overall, recovery was above 80% in all cases.

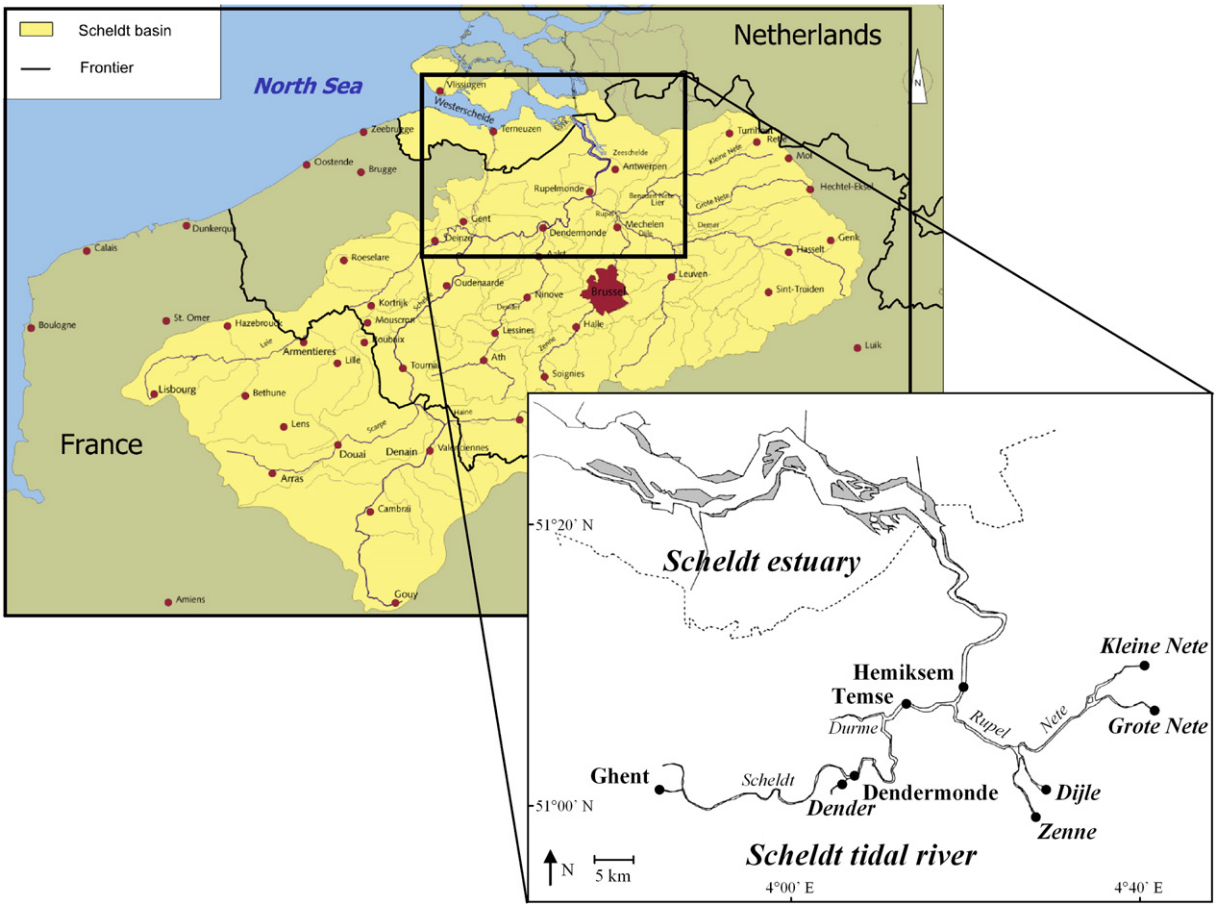

Fig. 1. Map of the Scheldt estuary and tidal river. The sampling stations (in bold) are indicated by black dots. City and river names are in regular and italic fonts, respectively. The dashed line follows the border between Belgium and The Netherlands. The insert displays the catchment area of the Scheldt and its tributaries (source: Schelde Informatie Centrum, www.scheldenet.nl).

Si isotopic compositions of DSi were then measured with a Nu Plasma MC–ICP–MS in dry plasma mode following Abraham et al. (2008). Mass bias was corrected through an external Mg doping. The sample-standard bracketing was used to correct for the long-term instrumental drift. All results (but one) have been measured as $\delta^{30}Si$ relative to NBS28 quartz standard (Table 1). Among the 36 new $\delta^{30}Si$ signatures provided in this study, 26 samples were replicated in different analytical sessions distributed over several months with an average standard deviation of duplicates of ±0.11‰ (±1 σ_{SD}) (Table 1). This is in agreement with the long-term reproducibility and accuracy of ±0.08‰ (±1 σ_{SD}) reported in Reynolds et al. (2007) and Abraham et al. (2008).

2.4. Isotopic and mass balance calculation

In order to evaluate the impact of the inputs of the tributaries on the isotopic signatures of the Scheldt tidal river, theoretical Si isotopic signatures that would have been obtained in the case of conservative mixing were estimated at Dendermonde [D] and at Hemiksem [H] ($\delta^{30}Si_{thmix\text{-}D}$ and $\delta^{30}Si_{thmix\text{-}H}$ respectively) by mass-balance calculations. They were compared respectively with those measured at Dendermonde ($\delta^{30}Si_D$) and at Hemiksem ($\delta^{30}Si_H$). Assuming that all the sources have been taken into account, same values should be obtained if conservative mixing was the only process affecting the isotopic signatures. The inputs considered for mass-balance calculations at Dendermonde were Ghent [G] and Dender [Dn], and those at Hemiksem were Temse [T] and the tributaries of the Rupel (Zenne [Z]–Dijle [Di]–Grote Nete [GN]–Kleine Nete [KN]):

$$\delta^{30}Si_{thmix-D} = \frac{\left(\delta^{30}Si_G \times F_G\right) + \left(\delta^{30}Si_{Dn} \times F_{Dn}\right)}{F_G + F_{Dn}} \quad (1)$$

$$\delta^{30}Si_{thmix-H} = \frac{\left(\delta^{30}Si_T \times F_T\right) + \left(\delta^{30}Si_Z \times F_Z\right) + \left(\delta^{30}Si_{Di} \times F_{Di}\right) + \left(\delta^{30}Si_{GN} \times F_{GN}\right) + \left(\delta^{30}Si_{KN} \times F_{KN}\right)}{F_T + F_Z + F_{Di} + F_{GN} + F_{KN}} \quad (2)$$

where

$$F_i = DSi_i \times Q_i \quad (3)$$

with $\delta^{30}Si_i$ denoting the Si isotopic composition of DSi measured at the sampling station [i] (in ‰), F_i the DSi flux at the station [i] (in mmol/s), DSi_i the DSi concentration at the station [i] (in μmol/l) and Q_i the (residual) water discharge at the station [i] (in m^3/s).

Table 1
The silicon isotope mass balance for 4 stations on the Scheldt River and the five tributaries during winter, spring, summer and fall.

	BSi (μmol/l)	DSi μmol/l	Discharge (Q) m^3/s	DSi Flux (F) mmol/s	f_{Si}	$\delta^{30}Si$ (‰) Measured	St. dev.	$\delta^{30}Si$ (‰) Calculated
WINTER-2003 (17–18th March)								
Ghent	14.2	231	35.2	8124	0.73	*1.46*	*0.08*	
Dender	3.3	220	13.5	2968	0.27	1.22	0.12	
Dendermonde	13.0	221	48.6	10,722		1.40	0.10	1.40
Temse	14.6	222	52.5	11,661	0.41	1.04	0.10	
Zenne	2.6**	286	8.2	2343	0.08	1.03	0.05	
Dijle	2.4**	301	33.5	10,071	0.36	0.79	0.08	
Grote Nete	4.5**	204	9.1	1858	0.07	0.90	0.19	
Kleine Nete	3.2**	216	10.4	2249	0.08	0.55	0.20	
Hemiksem	1.6	251	108.8	27,318		0.82	0.00	0.90
SPRING-2003 (26–27th May)								
Ghent	8.2	219	43.0	9404	0.83	1.19	0.05	
Dender	1.4	219	8.7	1902	0.17	*1.22*	*0.08*	
Dendermonde	37.4	201	51.7	10,395		1.23	0.00	1.19
Temse	21.9	179	56.8	10,173	0.41	1.22	0.14	
Zenne	2.6**	282	7.2	2033	0.08	0.96	0.02	
Dijle	1.1**	267	33.3	8899	0.36	1.03	0.03	
Grote Nete	3.8**	214	9.5	2029	0.08	*0.53*	*0.08*	
Kleine Nete	3.1**	183	10.4	1899	0.08	0.46	0.13	
Hemiksem	10.6	199	102.6	20,393		0.96	0.02	1.02
SUMMER-2008 (8th August)								
Ghent		215	75.4	16,211	0.82	*1.52*	*0.08*	
Dender		218	16.4	3575	0.18	*1.17*	*0.08*	
Dendermonde		39	92.1	3592		*2.09*	*0.08*	1.46
Temse		100	96.9	9690	0.31	0.97	0.25	
Zenne		263	19.0	4997	0.16	*1.03*	*0.08*	
Dijle		318	37.4	11,893	0.38	*1.18*	*0.08*	
Grote Nete		227	8.9	2020	0.07	*1.01*	*0.08*	
Kleine Nete		196	12.1	2372	0.08	0.80	0.24	
Hemiksem		96	174.2	16,723		*1.08*	*0.08*	1.05
FALL-2003 (27th October)								
Ghent	6.9	284	4.1	1165	0.54	1.16	0.21	
Dendre	1.7	238	4.1	975	0.46	1.09	0.03	
Dendermonde	151.8	188	8.2	1540		1.50	0.13	1.13
Temse	155.7	182	10.6	1930	0.15	1.33	0.09	
Zenne	3.0**	310	6.4	1986	0.15	1.09	0.17	
Dijle	1.7**	340	19.1	6490	0.50	0.78	0.13	
Grote Nete	4.0**	225	4.8	1081	0.08	0.99	0.00	
Kleine Nete	3.2**	156	9.0	1403	0.11	0.94	0.28	
Hemiksem	59.7	233	49.8	11,580		1.01*	0.02	0.95

f_{Si} is the ratio of DSi flux for each tributary over the sum of tributaries DSi fluxes upstream Dendermonde or in between Dendermonde and Hemiksem. St. dev. corresponds to the standard deviation of replicates.
Numbers in italics indicate no $\delta^{30}Si$ replication. In such case, average standard deviation of replicates is used: 0.08‰; 1 σ_{SD} (Abraham et al., 2008).
Discharge data presented here were calculated from raw data as in Carbonnel et al. (2009).
* For Hemiksem fall, $\delta^{30}Si$ has been calculated by converting $\delta^{29}Si$ into $\delta^{30}Si$ applying the kinetic mass fractionation factor of 1.96.
** These BSi concentrations were not directly measured but estimated using linear regressions versus the chlorophyll a ascribed to diatoms (Carbonnel et al., 2009). Note that they are only given here as rough indication due to the poor correlation coefficients, despite similar seasonal trends (Carbonnel et al., 2009). The annual average of the differences between measured and calculated BSi concentrations ranged from 50 to 80% of the annual average of the measured concentrations.

2.5. Models describing Si isotopes fractionation

There exist two simple models that are commonly applied to describe the variation of isotopic signature during the course of an uptake process which induces an isotopic fractionation (e.g. Fripiat et al., 2011): the Rayleigh model and the steady-state equilibrium model (also referred to as closed and open system models, respectively). One direct way to use these models is to compare measured $\delta^{30}Si$ with calculated $\delta^{30}Si$ of DSi following:

$$\text{Rayleigh} : \delta^{30}Si = \delta^{30}Si_0 + \varepsilon(\ln f_{Si}) \quad (4)$$

$$\text{Steady} - \text{state} : \delta^{30}Si = \delta^{30}Si_0 - \varepsilon(1 - f_{Si}) \quad (5)$$

where f_{Si} is the relative utilisation of the silicon reservoir downstream Ghent that can be calculated for example from the ratio of the DSi at Ghent (initial state) to that at Dendermonde (final state, cf. Section 4.3.2);ε represents the Si fractionation factor for diatoms relative to DSi expressed in per mil unit (-1.1 ± 0.4‰, De La Rocha et al., 1997; -1.1 ± 0.4‰ Alleman et al., 2005; -1.1 ± 0.2‰ Fripiat et al., 2011); $\delta^{30}Si_0$ is the isotopic signature of the Si source. In our study, the Si isotopic signature of DSi is calculated from conservative mixing at Dendermonde (Table 1).

Assuming that no other process than DSi consumption affect silicon during its transport from one station to another, and thus that the amount of BSi produced equals that of the DSi consumed, another equivalent way to use these models is to calculate how much BSi must have been produced to explain the changes in δ^{30}Si signatures by rewriting Eqs. (4) and (5) as:

$$\text{Rayleigh}: \quad \mathrm{BSi} = \mathrm{DSi} \times \left[\exp\left(\frac{\delta^{30}\mathrm{Si}_0 - \delta^{30}\mathrm{Si}}{\varepsilon} \right) - 1 \right] \tag{6}$$

$$\text{Steady} - \text{state}: \mathrm{BSi} = \mathrm{DSi} \times \left(\frac{\varepsilon}{\delta^{30}\mathrm{Si} - \delta^{30}\mathrm{Si}_0 + \varepsilon} - 1 \right). \tag{7}$$

Symbols are the same as in Eqs. (4) and (5).

3. Results

δ^{30}Si signatures in the Scheldt tidal river and in its tributaries vary by more than 1.50‰, ranging from +0.46‰ up to +2.09‰, with a mean value of $+1.05 \pm 0.35$‰ ($\pm 1\ \sigma_{SD}$) and exhibit significant spatial and seasonal variations (Fig. 2, Table 1). The δ^{30}Si seasonal variation of DSi, however differs depending on their geographical location (Table 1). The largest range of seasonal variation was observed in Dendermonde along the tidal river (up to 0.85‰) and the smallest one for the Zenne tributary (0.12‰).

The δ^{30}Si signatures measured in the Scheldt tidal river (mean + 1.25 ± 0.30‰, $\pm 1\ \sigma_{SD}$) are heavier than the ones found in the five tributaries (mean + 0.94 ± 0.22‰, $\pm 1\ \sigma_{SD}$). Moreover, our results also show a clear isotopic variation among tributaries: the average annual δ^{30}Si values decrease gradually from $+1.17 \pm 0.06$‰ ($\pm 1\ \sigma_{SD}$) for the Dender Basin to $+0.69 \pm 0.22$‰ ($\pm 1\ \sigma_{SD}$) for Kleine Nete Basin (Fig. 3). One of the most striking features is the large variation of δ^{30}Si signatures along the mainstream in winter (from +1.46‰ at Ghent down to +0.82‰ at Hemiksem) while DSi concentrations remain comparable (>200 µmol/l; Fig. 2).

The δ^{30}Si signatures calculated for the tidal river stations (Dendermonde, Hemiksem) making use of Eqs. (1) and (2) agree generally well with the observed ones (Table 1) suggesting that the isotopic variations observed in the Scheldt tidal river are driven by conservative mixing with those from the tributaries. There is however an exception for Dendermonde in summer 2008 and fall 2003 where the measured signatures are significantly heavier than calculated (+2.09‰ instead of +1.46‰ and +1.50‰ instead of +1.13‰, Table 1). These signatures correspond with a significant drop of DSi concentration when compared with the upstream locations Ghent and Dender (from 215/284 to 39/188 µmol·l^{-1} in 2008/2003 respectively; Table 1) that might be attributed to diatom blooms. The control of diatoms on Si isotopic signature at Dendermonde was estimated based on Eqs. (6) and (7) and assuming a conservative supply of the Dender tributary between Ghent (initial conditions, Table 2) and Dendermonde (Fig. 1).

Such setting of our system is allowed due to the short residence time of DSi which has been estimated to be 4.0 ± 1.7 days in this part of the Scheldt (Carbonnel et al., 2009). Ascribing this difference to DSi uptake by diatoms in between Ghent (initial state) and Dendermonde (final state) should yield to a δ^{30}Si signature of +3.34‰ (Rayleigh model) or +2.36‰ (steady state model) at Dendermonde (Table 2). The Rayleigh model is clearly not consistent with the measured value of $+2.09 \pm 0.06$‰ while the steady state model appears to be more realistic especially when taking into account an uncertainty of ± 0.2‰ on ε ($\pm 1\ \sigma_{SD}$; Fripiat et al., 2011), on which the calculated and measured values can be reconciled (Table 2).

The mean δ^{30}Si signature of DSi output from the Scheldt tidal river to the marine estuary (station Hemiksem; Fig. 1) was estimated to be $+0.95 \pm 0.02$‰ based on the four seasonal isotopic signatures, DSi concentrations and the river discharges Q as follows:

$$\Sigma \left[\frac{\delta^{30}\mathrm{Si} \times \mathrm{Q} \times \mathrm{DSi}}{\Sigma(\mathrm{Q} \times \mathrm{DSi})} \right] = \text{mean } \delta^{30}\mathrm{Si} \text{ export}. \tag{8}$$

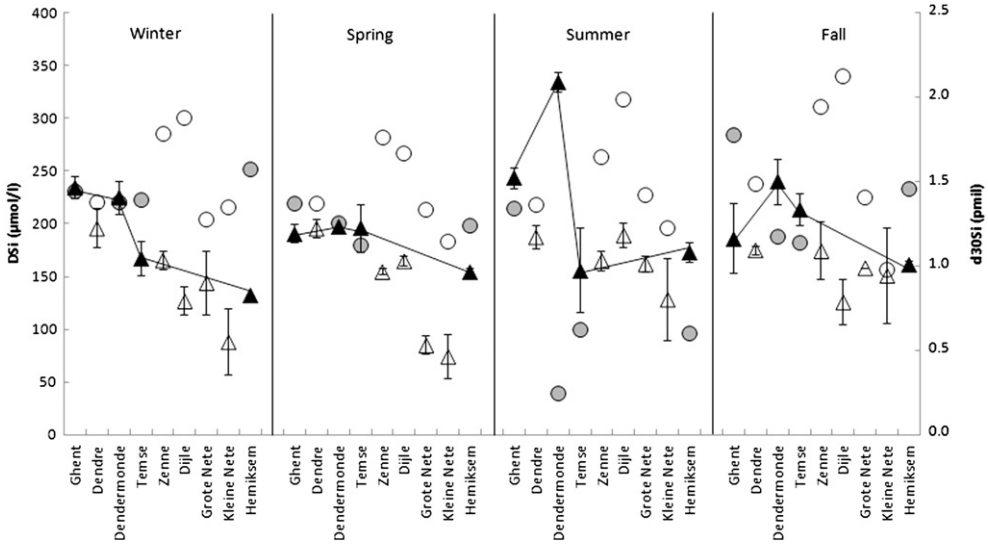

Fig. 2. Spatial and seasonal evolution of δ^{30}Si in the dissolved fraction and that of DSi concentrations. Data have been sorted from Ghent (left) downstream to Hemiksem (right). Filled circles: DSi concentration in the main Scheldt River. Open circles: DSi concentration in tributaries. Filled triangles connected with the black line: δ^{30}Si in main Scheldt River. Open triangles: δ^{30}Si in tributaries.

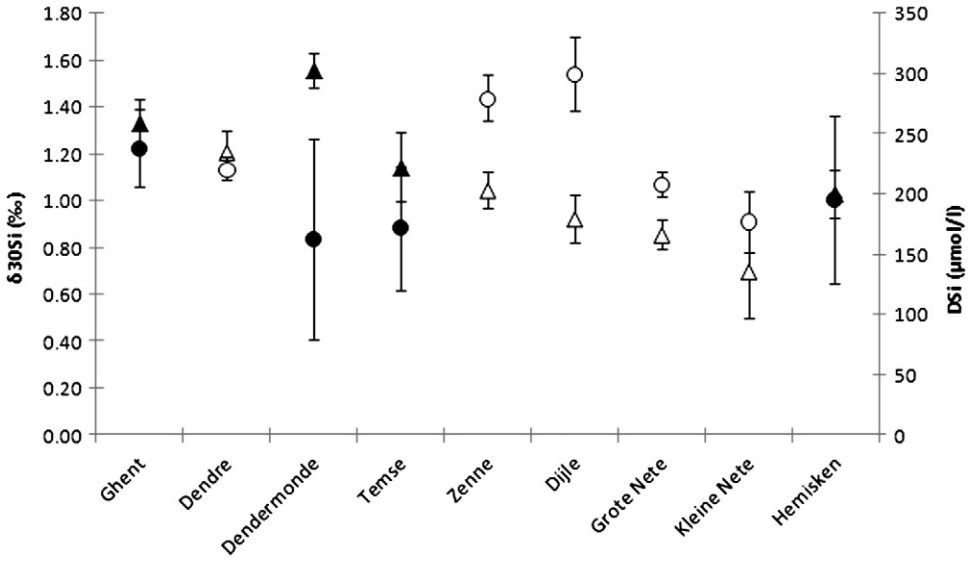

Fig. 3. Average annual $\delta^{30}Si$ (triangles) measured in the dissolved phase and average annual DSi concentrations (circles) from the five tributaries (open symbols) and from the Scheldt (filled symbols). Data have been sorted following stream, i.e. from Ghent (left) downstream to Hemiksem (right).

4. Discussion

4.1. Average $\delta^{30}Si$ signature in the Scheldt and comparison with other rivers

In this section, we discuss the mean tidal river value (+0.95‰) calculated by Eq. (8) which corresponds to the outlet of the Scheldt tidal river at Hemiksem upstream the saline estuary. We will discuss in other sections the seasonal and sub-basins variations. We should first acknowledge that the weighted annual average $\delta^{30}Si$ signature of the Scheldt at Hemiksem of $+0.95 \pm 0.02$‰ is calculated from four data only, assumed to be representative of each season. Nonetheless, the representativeness of the signature calculated from Eq. (8) is supported by the fact that the value calculated assuming conservative mixing is similar to the measured value at Hemiksem for each season (Table 1). The standard deviation of 0.02‰ has been calculated by simple propagation error on Eq. (8). It is low because the standard deviations of replicates for each of these four samples are particularly low (Table 1). It is likely that this standard deviation is underestimated compared to the actual mean average because of a potential bias due to under sampling of seasonal variation and mean analytical reproducibility around 0.08‰ (1 σ_{SD}; Abraham et al., 2008). Note that this 0.02‰ uncertainty should not be confounded with the intra-annual variability of the Scheldt signature. Actually, there can be large intra-annual variability with low uncertainty on the annual mean. We can evaluate the intra-annual variability of the $\delta^{30}Si$ signature by calculating the σ_{SD} of the 4 values, which amounts then to 0.11‰. Indeed, Hughes et al. (2011) report an uncertainty estimate of the same order (0.09‰, i.e. similar to the analytical standard error) on the mean annual $\delta^{30}Si$ signature of Congo River based on a 24-month monitoring. The weighted annual average of the Scheldt of $+0.95 \pm 0.02$‰ is close to the median value of riverine signatures published so far (1.09 ± 0.53‰ see compilation in Hughes et al., under revision) with the lightest measured in Iceland ($+0.63 \pm 0.38$‰, n = 25; Georg et al., 2007) and the heaviest measured in the Yangtze River ($+2.1 \pm 0.7$‰, n = 17; Ding et al., 2004). Although the Scheldt watershed is highly affected by anthropogenic activity, the mean annual $\delta^{30}Si$ signature in the tidal river is surprisingly comparable to that of a large pristine

Table 2
Estimates of the impact of diatom production on Si isotopic signature and BSi content at Dendermonde.

	DSi_0 (Ghent)	DSi	δ^{30}Si-M	$\delta^{30}Si_0$-C	ε	f_{Si}	δ^{30}Si Rayleigh	δ^{30}Si Steady	BSi-C Rayleigh	BSi-C Steady	BSi-M
Dendermonde Summer 2008	215	39	2.09	1.46	−1.3	0.18	3.68	2.52	24.3	36.6	90–250
Dendermonde Summer 2008	215	39	2.09	1.46	−1.1	0.18	3.34	2.36	30.1	52.2	90–250
Dendermonde Summer 2008	215	39	2.09	1.46	−0.9	0.18	3.00	2.20	39.5	91.0	90–250
Dendermonde Fall 2003	284	188	1.50	1.13	−1.3	0.66	1.67	1.57	61.8	74.7	150
Dendermonde Fall 2003	284	188	1.50	1.13	−1.1	0.66	1.58	1.50	75.1	95.2	150
Dendermonde Fall 2003	284	188	1.50	1.13	−0.9	0.66	1.50	1.43	95.5	131.1	150

All DSi and BSi concentrations are in µmol/l. All δ^{30}Si and ε are in ‰ relative to NBS28.
Initial condition is referred by 0 subscript and is represented by measured value. δ^{30}Si-M refers to measured δ^{30}Si at Dendermonde (Table 1).
$\delta^{30}Si_0$-C has been calculated from conservative mixing (Eq. (2) and Table 1).
f_{Si} is the ratio of DSi flux for each tributary over the sum of tributaries DSi fluxes upstream Dendermonde or in between Dendermonde and Hemiksem.
All calculated values are from Rayleigh (Eqs. (4) or (6)) or steady state (Eqs. (5) or (7)) models.
DSi_0 is the measured DSi contentration at Ghent.
ε and f_{Si} refer to parameters described in Eqs. (4)–(7).
For Summer 2008 and fall 2003 three values of fractionation factor have been tested.
See text for more details.

tropical river such as the Congo (+0.91 ± 0.09‰, n = 24; Hughes et al., 2011). Despite the fact that the Yangtze drains a temperate watershed with significant anthropogenic activities like the Scheldt, the average δ^{30}Si signatures are very different. In addition to possible analytical offsets on the Yangtze data raised by Georg et al. (2006) and supported by discrepancies in measurements of standards (Ding et al., 2005a; Reynolds et al., 2006; Valkiers et al., 2005), there are peculiarities in the study of Ding et al. (2004) compared to ours. The heavier isotopic signature of Yangtze has been partly attributed to rice cultures and damming. Rice is a silicon accumulating plant, especially in rice husks, which imposes an isotopic fractionation (Ding et al., 2005b); during harvest, this pool of isotopically light Si is removed from the watershed. This process has been shown to potentially explain the δ^{30}Si signatures of DSi in the Yangtze (Ding et al., 2008a). Damming also results in the preferential removal of light Si isotopes through diatoms' uptake and settling in reservoir lakes, a process also observed by Hughes et al. (2012). Damming is not an important process on the Scheldt watershed, and it seems that agriculture (ranging from 33 to 63% of land use, Table 3) has not resulted in heavier δ^{30}Si signatures at the Scheldt tidal river outlet either compared to pristine rivers. This can be due to the type and diversity of agriculture (compared to rice monoculture over the Yangtze watershed) and/or to the fact that several processes levelled off this impact on the mean Scheldt signature. Indeed we will see in Section 4.4.1 that land-use is likely to have a significant impact on river δ^{30}Si signature at the sub-basin scale.

4.2. Seasonal variations along the Scheldt tidal river

The δ^{30}Si signatures exhibit larger seasonal variations in the Scheldt tidal river (range of 0.85‰, Table 1) than those previously reported in Swiss rivers (range of 0.6‰; Georg et al., 2006). A recent study carried out near the estuary of the Kalix River (Sweden) also reported seasonal variations (from April to October) up to 0.8‰ for δ^{30}Si (Engström et al., 2010). Based on these results, Engström et al. (2010) also suggested that riverine DSi input to the ocean cannot be considered to have a constant Si isotopic composition on a short time-scale.

Our results for the Scheldt show that the seasonal variation observed at Dendermonde is large, but that it is reduced to a range of 0.16‰ at Hemiksem, the sampling station just upstream the saline estuary (Fig. 1). However, like at Dendermonde, DSi at Hemiksem can also be completely consumed by diatoms in river during dry years (Carbonnel et al., 2009), which would most probably result in a seasonal variation at Hemiksem as large as that at Dendermonde (see Section 4.3.2). Due to a higher discharge in the Rupel than in the Scheldt upstream the mouth of the Rupel, the complete consumption of DSi can last for a longer period at Dendermonde than at Hemiksem (Carbonnel et al., 2009). It is thus possible that in 2008, there has also been a period of complete DSi consumption, but as shown by our measured DSi concentration, we sampled outside this period. As a result, we cannot exclude the possibility that the seasonal variation at Hemiksem could in fact be higher than what was observed. This demonstrates that in order to determine the influence of rivers on the global oceanic Si isotopic composition, it is important to assess the seasonal variations of the isotopic signatures close to the estuary and at short time-scale. Moreover, DSi can also be significantly altered within saline estuaries (Chou and Wollast, 2006; Conley et al., 1993) and this is indeed the case for the Scheldt estuary (Carbonnel et al., in press; Soetaert et al., 2006). Unfortunately, the study of Si isotopes in estuaries has so far been neglected and there exists only few published estuarine data (Hughes et al., 2012). Overall the seasonal variations of the δ^{30}Si signatures in the tidal river seem to result from mixing with the tributaries and diatom's uptake. These processes are discussed in the following Section 4.3 while the variations among tributaries are discussed in Section 4.4.

4.3. Processes affecting δ^{30}Si signature in the tidal river

4.3.1. Mixing

Results obtained with the mass and δ^{30}Si balance model suggest that the isotopic signatures measured along the tidal river result mainly from the conservative mixing with lateral tributaries, with the exception of Dendermonde in summer and fall where diatom growth controls the signature (Section 4.3.2). This would imply that, except during bloom events, Si biogeochemical cycle within the Scheldt tidal river is not significantly affected by local biogeochemical processes that fractionate Si isotopes (uptake, dissolution, adsorption, precipitation…).

The generally lighter isotopic compositions of tributaries DSi are propagating along the tidal river after their confluence (Fig. 2). This is similar to what has been observed in the Congo Basin where the isotopic signature is heavier in the main branch (+1.22‰) than in the tributaries (+0.83‰) (Cardinal et al., 2010). The heavier δ^{30}Si signatures in the main stream are inherited from the area solely drained by the Scheldt upstream the city of Ghent. Such heavier isotopic signatures are also seen in the Dender. This probably results from the differences that exist between the western and the eastern parts of the Scheldt watershed as already highlighted for the Si biogeochemical cycle (Carbonnel et al., 2009). Such differences for Si isotopes will be discussed in Section 4.5.

The lightening of δ^{30}Si signature downstream Ghent is particularly important in winter when the δ^{30}Si signature is lowered by 0.64‰ between Ghent and Hemiksem while DSi concentrations remain high and comparable during a season when no significant biological activity and diatoms have been reported (Carbonnel et al., 2009). This highlights the leading role of the tributaries in determining the isotopic signature of the Scheldt tidal river and indicates that processes controlling the isotopic signature in the tidal part of the Scheldt River should be mostly located upstream. Such processes could not be assessed by simply looking at the DSi concentrations which remained rather constant in the tributaries (Carbonnel et al., 2009). They will be discussed in Section 4.4.

Table 3
Types of land-use (%). δ^{30}Si (‰) and DSi (μmol/l) in the five catchments.

Ecosystem	Dender %	Dijle %	Zenne %	Kleine Nete %	Grote Nete %	R^2 of correlation with δ^{30}Si	Sign of correlation	p-value
Permanent farming	0.0	2.1	0.0	0.1	0.0	0.00		0.98
Forest	3.2	11.2	6.3	21.4	17.4	0.95	−	<0.01
Grassland	11.1	4.0	6.8	15.8	19.2	0.25	−	0.39
Water surface	0.0	0.5	0.2	1.5	1.4	0.86	−	<0.05
Agricultural area*	62.9	53.3	47.2	37.9	33.6	0.70	+	<0.08
Wetland	0.0	0.2	0.0	0.5	0.3	0.89	−	0.02
Urban zone	22.7	28.7	39.5	22.7	28.0	0.05	+	0.73
δ^{30}Si (‰)	1.18	0.95	1.03	0.69	0.86			
DSi (μmol/l)	224	306	285	188	218			

Source: EEA-Corine Land Cover 2006.
δ^{30}Si and DSi are the average values of each tributary from Table 1.
* Correspond to “arable land” and “heterogeneous agricultural area” from the nomenclature of Corine Land Cover 2006.

4.3.2. Biogenic uptake

We measured the heaviest δ^{30}Si signatures of DSi at Dendermonde, +2.09‰ and +1.50‰, respectively in summer and fall. The δ^{30}Si ratios were respectively 0.53‰ and 0.37‰ heavier than those that would have been expected if there had been conservative mixing only. Such enrichment may be explained by diatom Si uptake. Diatom growth was significant in 2003 at Dendermonde, with summer BSi concentrations ranging from 90 to 250 μmol/l, reaching up to 350 μmol/l in fall, while DSi concentrations were below 10 μmol/l (Carbonnel et al., 2009). DSi depletion around Dendermonde is recurrent in summer (Muylaert et al., 2001, 2005; Soetaert et al., 2006; Struyf et al., 2004; Van Damme et al., 2005), depending on the river discharge. Indeed the low discharge of 2003 decreased DSi of the tidal river down to a few μmol/l (Carbonnel et al., 2009). The extent to which diatom growth can explain the measured shift in δ^{30}Si signature was estimated making use of Eqs. (6) and (7) and setting upstream and downstream boundaries at Ghent and Dendermonde respectively. We can set the initial conditions at Ghent and the final ones at Dendermonde because there, the residence time of DSi is 4 ± 1.7 days (Carbonnel et al., 2009). Calculated and measured BSi data were directly compared for fall 2003. In the absence of BSi data in summer 2008, the range of BSi observations during the summer 2003 was tentatively used (Carbonnel et al., 2009).

In fall 2003 at Dendermonde, the moderate enrichment in heavy isotope can be attributed to the moderate DSi decrease between Ghent (284 μmol/l) and Dendermonde (188 μmol/l) associated with a significant diatom bloom (BSi concentration at 150 μmol/l) (Carbonnel et al., 2009). From Eqs. (6) and (7) and taking into account the uncertainty on $^{30}\varepsilon$ (−1.1 ± 0.2‰; Fripiat et al., 2011), we calculated BSi concentrations of 62–95 μmol/l (Rayleigh, Table 2) or 75–131 μmol/l (steady-state, Table 2) to be compared to the value of 150 μmol/l measured by Carbonnel et al. (2009). The possible contribution of BSi originating from the Dender and the Scheldt at Ghent can be neglected since the concentrations at these stations were less than 10 μmol/l (Table 1; Carbonnel et al., 2009). The calculated BSi concentrations based on the Rayleigh model appear to be unrealistically low while those calculated from the steady-state model are in reasonable agreement with the BSi measured.

Overall, our calculations for fall 2003 confirm that the DSi consumption by diatoms can indeed be responsible for the shift in δ^{30}Si signatures that could not be explained by conservative mixing, and that the amount of diatoms present at Dendermonde can be high enough for such a shift in δ^{30}Si signatures. However, based on measured BSi concentrations in summer and fall 2003, the δ^{30}Si signatures should actually be heavier than the one measured.

BSi was not measured in 2008, but our calculated BSi concentrations using Rayleigh model appear to be fairly low (24–39 μmol/l; Table 2) compared to the ones measured in July–August 2003 (90–250 μmol/l; Carbonnel et al., 2009) and to the drawdown between DSi concentrations measured at Ghent and at Dendermonde in 2008 (Table 1). The fact that the Rayleigh model does not appear to be applicable to the system between Ghent and Dendermonde when diatom bloom is also logically observed; the calculated δ^{30}Si signatures of DSi are significantly heavier in summer 2008 compared to the measured one (>3‰ vs. 2.1‰, respectively Table 2). With the steady-state model, we nevertheless estimated higher BSi concentrations (36–91 μmol/l), but they would still be low compared to the ones measured in summer 2003. This can be indicative of:

(i) *Inter-annual variability of diatom blooms*. For summer 2008, while the DSi concentrations at Ghent and Dender were similar to those in 2003 (Table 1, Carbonnel et al., 2009), the DSi concentration at Dendermonde (39 μmol/l) was higher than that observed during the same period in summer 2003 (3 μmol/l; Carbonnel et al., 2009). This may be a consequence of the extremely warm 2003 summer in Europe (Garcia-Herrera et al., 2010). In the Scheldt tidal river, lower water discharge can indeed result in a stronger DSi depletion (Arndt et al., 2007; Carbonnel et al., 2009), which may explain the difference in DSi concentrations between the two summers.

(ii) *A temporal decoupling between BSi dynamics and isotopic signature of DSi*. This is however difficult to reconcile with the short water residence times during summer between Ghent and Dendermonde (4 ± 1.7 days; Carbonnel et al., 2009). Nevertheless, a possible decoupling between DSi and BSi dynamics in the Scheldt between Ghent and Dendermonde cannot be ruled out due to the presence of a local turbidity maximum at Dendermonde (Carbonnel et al., 2009; Chen et al., 2005). However, this would result in an enhanced retention of BSi at Dendermonde or upstream compared to that of the water (and of the DSi) and, in contradiction to our calculations, in BSi concentrations even higher than that the measured drawdown of DSi between Ghent and Dendermonde.

(iii) *Another Si source with a lighter Si isotopic composition of DSi might be missing in the budget calculation*. Such source could be the Durme River which has not been sampled in this study. However, it is unlikely that this small tributary could induce the Si isotopic shift observed since the Durme has a negligible discharge to the tidal river.

(iv) *A process involved in controlling δ^{30}Si signatures might have been neglected*. One of the most likely processes to take place is the dissolution of BSi. Demarest et al. (2009) have shown that dissolution of diatoms release preferentially light isotope with a Si fractionation factor for diatoms of −0.55‰ which should dampen the net isotopic fractionation. A dissolution-to-uptake ratio of 0.75 would yield a net fractionation factor of 0.8‰ (Demarest et al., 2009). The channel of the tidal river is bordered by mudflats and marshes, which account for 28% of the total surface of the tidal river system (Meire et al., 2005) and are preferential sites for BSi deposition and dissolution (Arndt and Regnier, 2007; Carbonnel et al., 2009). Although dissolution is not expected to be significant in the Scheldt tidal river on an annual timescale (Arndt and Regnier, 2007; Carbonnel et al., 2009), it may contribute significantly to sources of DSi to the tidal river during summer. The dissolution of BSi from the Scheldt tidal freshwater marshes could account for up to 50% of DSi concentrations in the tidal estuary during summer, when riverine discharges are reduced and when ambient DSi concentrations are low due to DSi consumption by diatoms (Arndt and Regnier, 2007; Struyf et al., 2005, 2006). This DSi, originating from BSi dissolution, is thus expected to exhibit lighter δ^{30}Si signatures compared to the DSi supplied by tributaries to the tidal river. This is consistent with the measured δ^{30}Si signatures that are lighter than the one expected based on the measured BSi concentration. This is also consistent with a steady state type of isotopic fractionation since such equilibrium fractionation can result from two reverse processes, each one inducting an isotopic fractionation (Fry, 2006). This process should however not affect our mass-balance calculations at Dendermonde as, upstream Dendermonde, the channel of the tidal river is almost completely canalised (Meire et al., 2005) and no BSi deposition is expected (Carbonnel et al., 2009).

Note that those processes involved to explain the discrepancy in 2008 could also be invoked for fall 2003. We acknowledge that our summer sampling is scarce and incomplete especially since BSi was not measured concomitantly with DSi in 2008. This prevents us from going further into the discussion. Nevertheless, our results would suggest that dissolution process is most likely the mechanism that would explain a δ^{30}Si signature lighter than expected in diatoms bloom period.

4.4. Difference among tributaries and controlling factors

Diatoms hardly bloomed in the tributaries: throughout the year, DSi concentrations stayed high and BSi concentrations remained low

(generally below 10 μmol/l, and only up to 30 μmol/l in the Dender in spring and summer 2003, and probably in the Zenne in spring 2003; Carbonnel et al., 2009). Based on this rather homogeneous elevated DSi and low BSi measured in the different tributaries, it is assumed that the observed inter-tributary isotopic signature could not be primarily attributed to biological processes and is rather catchment specific. This was investigated by plotting the tributary isotopic signatures as function of 1/DSi (Fig. 4). A positive linear correlation in such a diagram is indicative of a mixing process between two end-members (Fry, 2006). The intercept identifies the isotopic composition of the ultimate Si-rich source while the other end-member would be representative of waters that are Si-depleted and enriched in heavier isotopes due to a fractionation process. In the plot of the Dijle, Zenne and Dender the linear trend suggests similar source and process controls for these three sub-basins. While the much larger scattering in the plots for the Kleine and Grote Nete demonstrates that more complex factors control the Si content in those two rivers.

4.4.1. The Dijle Zenne and Dender tributaries

This group of rivers show increasing δ^{30}Si signatures with increasing 1/DSi, i.e. with decreasing DSi concentration ($R^2 = 0.45$; p-value < 0.02, Fig. 4). This likely traces back a process of clay neoformation in the groundwater seeping zone. Indeed, clay formation during the weathering process releases DSi into soil solution and since light isotopes are preferentially incorporated into clays (e.g. Opfergelt et al., 2010; Ziegler et al., 2005), Si released into soil waters is enriched in heavy isotopes. It is noteworthy that this negative correlation between DSi and δ^{30}Si ratio is opposite to what is generally observed in rivers which is usually explained by a complex interplay between δ^{30}Si, weathering intensity and type of secondary mineral formed (Cardinal et al., 2010; De La Rocha et al., 2000; Georg et al., 2006; Hughes et al., 2012, under revision). The positive correlation between δ^{30}Si and 1/DSi might be indicative of Si release from a isotopic light reservoir such as clays or congruent dissolution from primary minerals (Cardinal et al., 2010; Cornelis et al., 2010; Hughes et al., under revision) as discussed in Section 4.4.2 and/or land-use as discussed in Section 4.5.

4.4.2. The Grote and Kleine Nete

The Kleine Nete catchment area is mainly located over sandy aquifer (e.g. Vanlierde et al., 2007) in contrast to the Dender, Zenne and Dijle basins which develop in aquifers with higher clay contents (Marechal, 1992). The lighter isotopic compositions of the Si source within the Kleine Nete aquifer cannot be linked to the sandy component since the signature of quartz should be around 0‰ (André et al., 2006). However, these sandy aquifers contain very high quantities of glauconites, a clay-like phyllosilicate which is extensively dissolved within the aquifer ensuring substantial amounts of Fe^{2+} within the aquifers. Since these glauconites are secondary clays, we may expect them to present negative Si isotopic signatures. The extensive glauconite dissolution is a likely explanation for the lighter δ^{30}Si signature of the Kleine Nete tributary along with land use (see discussion in Section 4.5) and may also have another effect on Si isotopic composition: lightest silicon isotopes would be preferentially adsorbed on the substantial quantities of authigenic iron minerals (Delstanche et al., 2009) that would precipitate and flocculate when the groundwater under reduced environment enters the surface water system, (Vanlierde et al., 2007). Such process could be specific to the Kleine Nete and explain the isotopic shift observed in Fig. 4 (and in a less extent to Grote Nete, see below). However, the other usual processes in the soil–plant–river continuum would also be occurring to set positive δ^{30}Si signatures in the Kleine Nete.

Finally, it is worth noting that the Grote Nete of which the samples are located in between those of the Kleine Nete and those of the group formed by Dender, Zenne and Dijle tributaries regards to the δ^{30}Si versus 1/DSi plots (Fig. 4), is also situated in between these two (group of) rivers both geographically and lithologically.

4.5. Role of plants and land use

In terrestrial environments, higher plants can affect the hydrological output of DSi not only through root-induced silicate weathering but also through Si uptake and BSi restitution via its litterfall (Alexandre et al., 1997). During the growing season, vegetation takes up most of the DSi made available by weathering of soil minerals (and by phytolith dissolution), and converts it into phytoliths (back), a large fraction of which will return to the soils in litter (Farmer et al., 2005). This BSi restitution can largely contributes to DSi release to soil waters and ultimately to rivers (Struyf et al., 2010).

Plants preferentially take up light Si isotopes, leaving heavier δ^{30}Si signatures in the soil water (e.g. Opfergelt et al., 2006; Ziegler et al., 2005). The δ^{30}Si signature of phytoliths could be in addition impacted

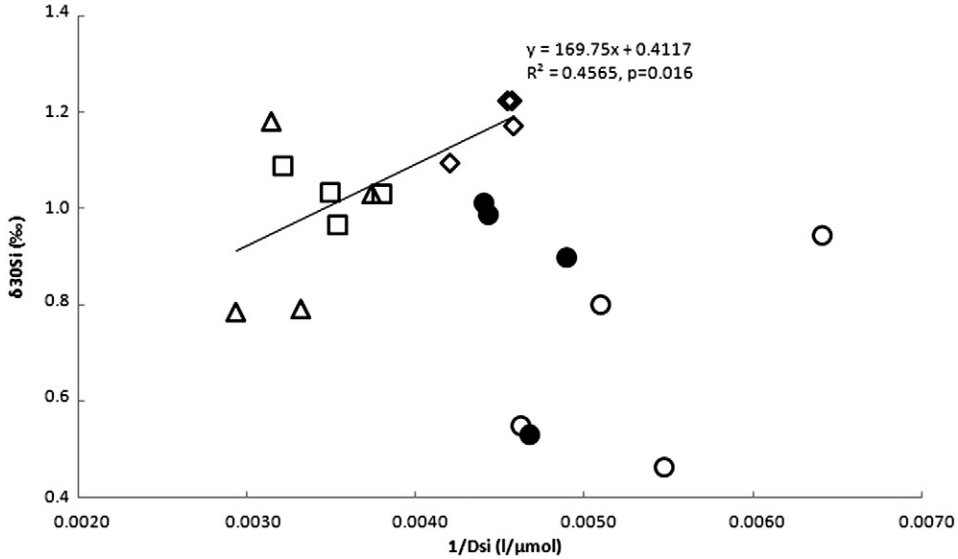

Fig. 4. δ^{30}Si signatures (‰) in the tributaries as a function of 1/DSi (l/μmol). Dijle (triangles), Zenne (squares), Dender (diamonds), Grote Nete (filled circles) and Kleine Nete (open circles). Correlation line has been calculated on Dijle, Zenne and Dender data (i.e. excluding Grote Nete and Kleine Nete).

by the degree of soil weathering (Opfergelt et al., 2008). When the soil–plant system is in steady-state, one would expect no change in the DSi content but gradually heavier signatures with the increase of the fraction of neoformed clays within the soils at geological time scales. The turnover might be species dependent as plants differ greatly in their ability to accumulate Si in their aerial parts, ranging from 0.1 to 10% of their dry weight (Gerard et al., 2008; Hodson et al., 2005; Vandervorm, 1980). Hence, the cycling should be larger for monocotyledons than dicotyledons because the former incorporates significantly more Si than the latter, implying that the turnover could be different in forest relative to grassland and croplands.

Recent studies by Ding et al. (2004, 2008a) have provided support that crops could imbalance the Si cycle by giving rise to isotopically heavier and DSi-depleted river signatures due to phytoliths formation and their subsequent removal from the soil–plant system during harvest.

Therefore, in addition to the lithological variation, a land-use variation may also partly explain the different isotopic signatures. It is noteworthy that the percentage of forest cover in the Dijle basin (11%) is four times larger compared to the Dender basin (3%) and it is two times larger in the Kleine and Grote Nete (21 and 17% respectively) basins compared to Dijle basin. Indeed, the highest (negative) correlation coefficient (Fig. 5 and Table 3) is observed between the extent of forest coverage and the average δ^{30}Si values ($R^2 = 0.95$, $n = 5$, p-value<0.01). This is consistent with a lighter δ^{30}Si resulting from enhanced clay dissolution due to high organic matter contents and lower pH in soils of forested regions (Cardinal et al., 2010; Cornelis et al., 2010). Engström et al. (2010) have reported a negative correlation between δ^{30}Si signature and forest cover, which is also in agreement with our results.

Despite their extremely small fraction of the land cover (<1.5%), the wetland and water surface coverages are also highly anti-correlated with δ^{30}Si ($R^2 = 0.90$ and 0.84 respectively, p-values<0.05). At first sight, this may appear to be in complete contradiction with Engström et al. (2010) who reported a positive correlation between lake cover and river δ^{30}Si in Sweden. The latter probably results from a significant diatom uptake occurring in lake ecosystems. However, considering that lakes do not constitute the main part of water bodies in the Scheldt watershed, which are rather dominated by wetlands, both studies can be reconciled. As already stated, in the Scheldt watershed, there exists an important pool of wetlands where significant BSi dissolution takes place (Struyf et al., 2004, 2005, 2006). Although this process is different from clay dissolution favoured by the presence of humic acids in forested area, both should result in lighter δ^{30}Si values in DSi and appear to be major features controlling the difference in δ^{30}Si signatures of the Scheldt tributaries.

In addition, the agriculture area covers a large part of the tributary catchments (33.6 to 62.9%), with a coefficient correlation with δ^{30}Si of 0.68 (p-value<0.08; Table 3). Even if this r^2 is lower and p-value higher than the ones obtained with wetland and forest areas, this type of land-use could partly control river DSi isotopic signatures. Indeed, the Dender basin has a high percentage of grasslands and croplands (including arable land, agricultural area and permanent farming) and is associated with a heavier δ^{30}Si signature, which might then be explained by the removal of phytoliths (light Si) from the ecosystem during harvest (Ding et al., 2004; Ding et al., 2008a,b). These results indicate that land-use can be a major player in controlling some riverine silicon isotopic compositions. Struyf et al. (2010) have shown recently that silica fluxes are impacted by anthropogenic changes of land-use in the Scheldt River Basin.

We note however that urban zone does not explain in any noticeable way the variations of riverine δ^{30}Si measured in the different tributaries of the Scheldt watershed. This is in agreement with a study showing the limited impact of direct anthropogenic pressures (sewage, industry…) on the Si cycle in a comparable river system (Seine, France; Sferratore et al., 2006). However, since the percentages of land-use cover are not independent of each other, we cannot from these data quantify the individual contribution of each type of land-use to the average δ^{30}Si river signature. Further studies should thus focus more specifically on this aspect.

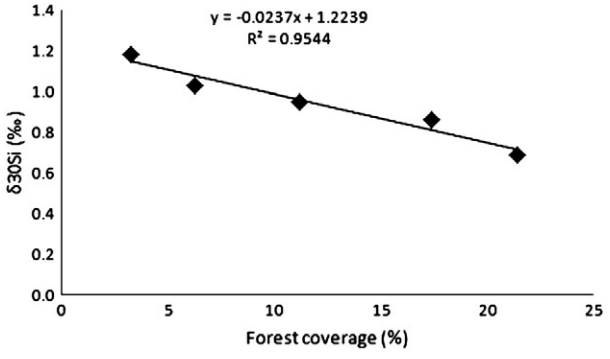

Fig. 5. Correlation between the extent of forest coverage (%) and the average δ^{30}Si values (‰) of the five catchments.

5. Conclusion

We report the first seasonal variations of riverine δ^{30}Si signatures at the Scheldt tidal river and its tributary outlets, a temperate watershed that is highly impacted by anthropic activities. Our results show that (i) Except for large diatom bloom events which are limited to some of the summer and fall periods in the tidal river, the processes controlling δ^{30}Si signatures are most likely to take place upstream the freshwater tidal river, i.e. within the sub-basins of the tributaries. (ii) Large variations of δ^{30}Si signatures in non-bloom periods can be observed even when DSi concentration remains relatively constant. This supports the use of δ^{30}Si as a sensitive tool to track sources and processes involved in the continental biogeochemical silicon cycle. (iii) In the tidal river the diatom blooms induce a large increase in δ^{30}Si signatures. However, the actual isotopic shift induced by diatom uptake might be partly dampened by the significant dissolution in summer and fall of biogenic silica of wetland and/or diatom origins. (iv) Land-use, more specifically the extent of forest and wetland covers, seems to be the main factor explaining the differences in δ^{30}Si values of tributaries in the Scheldt, i.e. at the sub-basin level. Both types give rise to lighter δ^{30}Si signatures of the DSi. For forest, this confirms that the Si isotopic composition of DSi set initially by clay formation can be altered by its re-dissolution due to the presence of dissolved organic matter, which leads to a decrease in the δ^{30}Si signature of the DSi exported to rivers (Cardinal et al., 2010; Cornelis et al., 2010). For wetland, it is likely that such environment supplies isotopically lighter DSi as a result of BSi dissolution (Struyf et al., 2004, 2005, 2006) and associated fractionation (Demarest et al., 2009; Ziegler et al., 2005;). Lithology and agricultural activity might also important factors affecting the δ^{30}Si signature while the impact of urban zone seems to be negligible both at the sub-basin and whole watershed scales. (v) Indeed at the outlet, the significant sub-basin differences in land-use and lithology are levelled off which probably explain why δ^{30}Si signatures at Hemiksem display a much smaller seasonal variation and a mean δ^{30}Si at $+0.95$‰ that compared well to the world average. (vi) By modifying land-use, anthropogenic activities have altered the Si biogeochemical cycle in the Scheldt Basin (Struyf et al., 2010) and such changes may also modify the Si isotopic composition of DSi in rivers. It has recently been observed that an anthropogenic pressure such as damming and agriculture alters the riverine δ^{30}Si signatures (Ding et al., 2008a,b; Hughes et al., 2012), but the impact of land-use change needs to be confirmed by appropriate seasonal monitoring of others rivers. It would be particularly interesting to focus on a number of selected rivers under different climate regimes, lithological settings, land-use and anthropogenic pressures.

Acknowledgements

We would like to thank N. Canu, R. Dasseville, M. Lionard, Ch. de Marneffe, N. Roevros, M. Tsagaris and S. Vanneste for their assistance in field sampling during 2003 as well as in laboratory analyses. Water discharge data were provided by the Flanders Hydraulics Research, Hydrological Information Centre. This study was conducted in the framework of the TIMOTHY project financed by the Belgian Federal Science Policy Office (BELSPO) under contract number "Interuniversity Attraction Pole IAP 6/13". The 2003 sampling programme was carried out within the framework of the SISCO project also financed by BELSPO (contract number EV/11/17A). Thanks to F. Planchon for support in the summer 2008 sampling. The Fonds National de la Recherche Scientifique provided the funding of the Nu Plasma Multi-Collector Mass Spectrometer facility (FRFC 2.4579.04) at Université Libre de Bruxelles. N. Mattielli and J. de Jong (ULB) are warmly thanked for the management of the MC–ICP–MS. Two anonymous reviewers are gratefully acknowledged for their constructive comments and suggestions which improved the clarity of this paper.

References

Abraham, K., Opfergelt, S., Fripiat, F., Cavagna, A.J., de Jong, J.T.M., Foley, S.F., Andre, L., Cardinal, D., 2008. delta Si-30 and delta Si-29 determinations on USGS BHVO-1 and BHVO-2 reference materials with a new configuration on a nu plasma multi-collector ICP–MS. Geostand. Geoanal. Res. 32, 193–202.

Alexandre, A., Meunier, J.D., Colin, F., Koud, J.M., 1997. Plant impact on the biogeochemical cycle of silicon and related weathering processes. Geochim. Cosmochim. Acta 61, 677–682.

Alleman, L.Y., Cardinal, D., Cocquyt, C., Plisnier, P.D., Descy, J.P., Kimirei, I., Sinyinza, D., André, L., 2005. Silicon isotopic fractionation in Lake Tanganyika and its main tributaries. J. Great Lakes Res. 31, 509–519.

André, L., Cardinal, D., Alleman, L.Y., Moorbath, S., 2006. Silicon isotopes in 3.8 Ga West Greenland rocks as clues to the Eoarchaean supracrustal Si cycle. Earth Planet. Sci. Lett. 245, 162–173.

Arndt, S., Regnier, P., 2007. A model for the benthic–pelagic coupling of silica in estuarine ecosystems: sensitivity analysis and system scale simulation. Biogeosciences 4, 331–352.

Arndt, S., Vanderborght, J.-P., Regnier, P., 2007. Diatom growth response to physical forcing in a macrotidal estuary: coupling hydrodynamics, sediment transport, and biogeochemistry. J. Geophys. Res. 112, C05045.

Belanger, R.R., Benhamou, N., Menzies, J.G., 2003. Cytological evidence of an active role of silicon in wheat resistance to powdery mildew (*Blumeria graminis* f. sp. *tritici*). Phytopathology 93, 402–412.

Canfield, D.E., Kristensen, E., Thamdrup, B., 2005. The silicon cycle. Aquat. Geomicrobiol. 48, 441–463.

Carbonnel, V., Lionard, M., Muylaert, K., Chou, L., 2009. Dynamics of dissolved and biogenic silica in the freshwater reaches of a macrotidal estuary (The Scheldt, Belgium). Biogeochemistry 96, 49–72.

Carbonnel, V., Vanderborght, J.P., Lionard, M., Chou, L., in press. Diatoms, silicic acid and biogenic silica dynamics along the salinity gradient of the Scheldt estuary (Belgium/The Netherlands). Biogeochemistry (http://dx.doi.org/10.1007/s10533-012-9796-y).

Cardinal, D., Alleman, L.Y., de Jong, J., Ziegler, K., André, L., 2003. Isotopic composition of silicon measured by multicollector plasma source mass spectrometry in dry plasma mode. J. Anal. At. Spectrom. 18, 213–218.

Cardinal, D., Gaillardet, J., Hughes, H.J., Opfergelt, S., André, L., 2010. Contrasting silicon isotope signatures in rivers from the Congo Basin and the specific behaviour of organic-rich waters. Geophys. Res. Lett. 37, L12403.

Chen, M.S., Wartel, S., Van Eck, B., Van Maldegem, D., 2005. Suspended matter in the Scheldt estuary. Hydrobiologia 540 (1–3), 79–104.

Chou, L., Wollast, R., 2006. Estuarine silicon dynamics. In: Ittekkot, V., Unger, D., Humborg, C., Tac An, N. (Eds.), The Silicon Cycle. Human Perturbation and Impacts on Aquatic Systems. Island Press, Washington, Covelo, London, pp. 93–120.

Conley, D.J., 2002. Terrestrial ecosystems and the global biogeochemical silica cycle. Global Biogeochem. Cycles 16.

Conley, D.J., Schelske, C.L., Stoermer, E.F., 1993. Modification of the biogeochemical cycle of silica with eutrophication. Mar. Ecol. Prog. Ser. 101, 179–192.

Cornelis, J.T., 2010. Impact of tree species on silicon cycling in temperate soil–tree systems. PhD, Université Catholique de Louvain.

Cornelis, J.T., Delvaux, B., Cardinal, D., André, L., Ranger, J., Opfergelt, S., 2010. Tracing mechanisms controlling the release of dissolved silicon in forest soil solutions using Si isotopes and Ge/Si ratios. Geochim. Cosmochim. Acta 74, 3913–3924.

Cox, T.J.S., Maris, T., Soetaert, K., Conley, D.J., Van Damme, S., Meire, P., Middelburg, J.J., Vos, M., Struyf, E., 2009. A macro-tidal freshwater ecosystem recovering from hypereutrophication: the Schelde case study. Biogeosciences 6, 2935–2948.

De La Rocha, C.L., Brzezinski, M.A., DeNiro, M.J., 1996. Purification, recovery, and laser-driven fluorination of silicon from dissolved and particulate silica for the measurement of natural stable isotope abundances. Anal. Chem. 68, 3746–3750.

De La Rocha, C.L., Brzezinski, M.A., DeNiro, M.J., 1997. Fractionation of silicon isotopes by marine diatoms during biogenic silica formation. Geochim. Cosmochim. Acta 61, 5051–5056.

De la Rocha, C.L., Brzezinski, M.A., DeNiro, M.J., 2000. A first look at the distribution of the stable isotopes of silicon in natural waters. Geochim. Cosmochim. Acta 64, 2467–2477.

Delstanche, S., Opfergelt, S., Cardinal, D., Elsass, F., André, L., Delvaux, B., 2009. Silicon isotopic fractionation during adsorption of aqueous monosilicic acid onto iron oxide. Geochim. Cosmochim. Acta 73, 923–934.

Demarest, M.S., Brzezinski, M.A., Beucher, C.P., 2009. Fractionation of silicon isotopes during biogenic silica dissolution. Geochim. Cosmochim. Acta 73, 5572–5583.

Derry, L.A., Kurtz, A.C., Ziegler, K., Chadwick, O.A., 2005. Biological control of terrestrial silica cycling and export fluxes to watersheds. Nature 433, 728–731.

Ding, T., Wan, D., Wang, C., Zhang, F., 2004. Silicon isotope compositions of dissolved silicon and suspended matter in the Yangtze River, China. Geochim. Cosmochim. Acta 68, 205–216.

Ding, T., Wan, D., Bai, R., Zhang, Z., Shen, Y., Meng, R., 2005a. Silicon isotope abundance ratios and atomic weights of NBS-28 and other reference materials. Geochim. Cosmochim. Acta 69 (23), 5487–5494.

Ding, T.P., Ma, G.R., Shui, M.X., Wan, D.F., Li, R.H., 2005b. Silicon isotope study on rice plants from the Zhejiang province, China. Chem. Geol. 218, 41–50. http://dx.doi.org/10.1016/j.gca.2005.06.015.

Ding, T.P., Tian, S.H., Sun, L., Wu, L.H., Zhou, J.X., Chen, Z.Y., 2008a. Silicon isotope fractionation between rice plants and nutrient solution and its significance to the study of the silicon cycle. Geochim. Cosmochim. Acta 72, 5600–5615.

Ding, T.P., Zhou, J.X., Wan, D.F., Chen, Z.Y., Wang, C.Y., Zhang, F., 2008b. Silicon isotope fractionation in bamboo and its significance to the biogeochemical cycle of silicon. Geochim. Cosmochim. Acta 72, 1381–1395.

Dougan, W.K., Wilson, A.L., 1974. The absorptiometric determination of aluminium in water. A comparison of some chromogenic reagents and the development of an improved method. Analyst 99, 413–430.

Engström, E., Rodushkin, I., Ingri, J., Baxter, D.C., Ecke, F., Osterlund, H., Ohlander, B., 2010. Temporal isotopic variations of dissolved silicon in a pristine boreal river. Chem. Geol. 271, 142–152.

Epstein, E., 1999. Silicon. Annu. Rev. Plant Physiol. Plant Mol. Biol. 50, 641–664.

Farmer, V.C., Delbos, E., Miller, J.D., 2005. The role of phytolith formation and dissolution in controlling concentrations of silica in soil solutions and streams. Geoderma 127, 71–79.

Fripiat, F., Cavagna, A.J., Savoye, N., Dehairs, F., André, L., Cardinal, D., 2011. Isotopic constraints on the Si-biogeochemical cycle of the Antarctic Zone in the Kerguelen area (KEOPS). Mar. Chem. 123, 11–22.

Fry, B., 2006. Stable Isotope Ecology. Springer, New York.

Garcia-Herrera, R., Diaz, J., Trigo, R.M., Luterbacher, J., Fischer, E.M., 2010. A review of the European summer heat wave of 2003. Crit. Rev. Environ. Sci. Technol. 40, 267–306.

Georg, R.B., Reynolds, B.C., Frank, M., Halliday, A.N., 2006. Mechanisms controlling the silicon isotopic compositions of river waters. Earth Planet. Sci. Lett. 249, 290–306.

Georg, R.B., Reynolds, B.C., West, A.J., Burton, K.W., Halliday, A.N., 2007. Silicon isotope variations accompanying basalt weathering in Iceland. Earth Planet. Sci. Lett. 261, 476–490. http://dx.doi.org/10.1016/j.epsl.2007.07.004.

Gerard, F., Mayer, K.U., Hodson, M.J., 2008. Modelling the biogeochemical cycle of silicon in soils: application to a temperate forest ecosystem. Geochim. Cosmochim. Acta 72, 741–758.

Hodson, M.J., White, P.J., Mead, A., Broadley, M.R., 2005. Phylogenetic variation in the silicon composition of plants. Ann. Bot. 96, 1027–1046.

Hughes, H.J., Sondag, F., Cocquyt, C., Laraque, A., Pandi, A., Andre, L., Cardinal, D., 2011. Effect of seasonal biogenic silica variations on dissolved silicon fluxes and isotopic signatures in the Congo River. Limnol. Oceanogr. 56, 551–561.

Hughes, H.J., Bouillon, S., André, L., Cardinal, D., 2012. The effects of weathering variability and anthropogenic pressures upon silicon cycling in an intertropical watershed (Tana River, Kenya). Chem. Geol. 308–309, 18–25.

Hughes, H.J., Sondag, F., André, L., Cardinal, D. The global silicon isotope composition of rivers: new insights from the Amazon Basin and the world database. Under revision for Geochimica Cosmochimica Acta.

Koroleff, F., 1983. Determination of Silicon. Methods of Seawater Analysis. In: Grasshoff, K., Ehrhardt, M., Kremling, K. (Eds.), Second, Revised and Extended Edition. Verslag Chemie, Weinheim, Deerfield Beach, Florida, Basel, pp. 174–187.

Lancelot, C., 1995. The mucilage phenomenon in the continental coastal waters of the North-Sea. Sci. Total. Environ. 165, 83–102.

Marechal, R., 1992. Deuxième atlas de Belgique. Géologie du quaternaire - Lithologie des terrains superficiels. Planche II.3.1-2 au 1:250,000. Institut Géographique National, Bruxelles.

Martin-Jézéquel, V., Hildebrand, M., Brzezinski, M.A., 2000. Silicon metabolism in diatoms: implications for growth. J. Phycol. 36, 821–840.

Meire, P., Ysebaert, T., Van Damme, S., Van den Bergh, E., Maris, T., Struyf, E., 2005. The Scheldt estuary: a description of a changing ecosystem. Hydrobiologia 540, 1–11.

Meunier, J.D., Kirman, S., Strasberg, D., Nicolini, E., Delcher, E., Keller, C., 2010. The output and bio-cycling of Si in a tropical rain forest developed on young basalt flows (La Reunion Island). Geoderma 159, 431–439.

Muylaert, K., Van Wichelen, J., Sabbe, K., Vyverman, W., 2001. Effects of freshets on phytoplankton dynamics in a freshwater tidal estuary (Schelde, Belgium). Arch. Hydrobiol. 150, 269–288.

Muylaert, K., Tackx, M., Vyverman, W., 2005. Phytoplankton growth rates in the freshwater tidal reaches of the Schelde estuary (Belgium) estimated using a simple light-limited primary production model. Hydrobiologia 540, 127–140.

Officer, C.B., Ryther, J.H., 1980. The possible importance of silicon in marine eutrophication. Mar. Ecol. Prog. Ser. 3, 83–91.
Opfergelt, S., Cardinal, D., Henriet, C., Draye, X., André, L., Delvaux, B., 2006. Silicon isotopic fractionation by banana (*Musa* spp.) grown in a continuous nutrient flow device. Plant Soil 285, 333–345.
Opfergelt, S., Delvaux, B., André, L., Cardinal, D., 2008. Plant silicon isotopic signature might reflect soil weathering degree. Biogeochemistry 91, 163–175.
Opfergelt, S., Cardinal, D., André, L., Delvigne, C., Bremond, L., Delvaux, B., 2010. Variations of δ^{30}Si and Ge/Si with weathering and biogenic input in tropical basaltic ash soils under monoculture. Geochim. Cosmochim. Acta 74, 225–240.
Passy, P., Gypens, N., Billen, G., Garnier, J., Thieu, V., Rousseau, V., Callens, J., Parent, J.-Y., Lancelot, C., et al., 2013. A model reconstruction of riverine nutrient fluxes and eutrophication in the Belgian Coastal Zone since 1984. J. Mar. Syst. 128, 106–122 (this volume).
Ragueneau, O., Treguer, P., Leynaert, A., Anderson, R.F., Brzezinski, M.A., DeMaster, D.J., Dugdale, R.C., Dymond, J., Fischer, G., Francois, R., Heinze, C., Maier-Reimer, E., Martin-Jezequel, V., Nelson, D.M., Queguiner, B., 2000. A review of the Si cycle in the modem ocean: recent progress and missing gaps in the application of biogenic opal as a paleoproductivity proxy. Glob. Planet. Chang. 26, 317–365.
Ragueneau, O., Conley, D.J., Leynaert, A., Ni Longphuirt, S., Slomp, C.P., 2006. Role of diatoms in silicon cycling and coastal marine food webs. In: Ittekot, V., Unger, D., Humborg, C., An, N.T. (Eds.), The Silicon Cycle. Human Perturbations and Impacts on Aquatic Systems. Island Press, Washington, Covelo, London, pp. 163–195.
Reynolds, B.C., Georg, R.B., Oberli, F., Wiechert, U., Halliday, A.N., 2006. Re-assessment of silicon isotope reference materials using high-resolution multi-collector ICP–MS. J. Anal. At. Spectrom. 21 (3), 266. http://dx.doi.org/10.1039/b515908c.
Reynolds, B.C., Aggarwal, J., André, L., Baxter, D., Beucher, C., Brzezinski, M.A., Engstrom, E., Georg, R.B., Land, M., Leng, M.J., Opfergelt, S., Rodushkin, I., Sloane, H.J., van den Boorn, S.H.J.M., Vroon, P.Z., Cardinal, D., 2007. An inter-laboratory comparison of Si isotope reference materials. J. Anal. At. Spectrom. 22, 561–568.
Reynolds, O.L., Keeping, M.G., Meyer, J.H., 2009. Silicon-augmented resistance of plants to herbivorous insects: a review. Ann. Appl. Biol. 155, 171–186.
Sferratore, A., Garnier, J., Billen, G., Conley, D.J., Pinault, S., 2006. Diffuse and point sources of silica in the Seine River Watershed. Environ. Sci. Technol. 40–21, 6630–6635.
Soetaert, K., Middelburg, J.J., Heip, C., Meire, P., Van Damme, S., Maris, T., 2006. Long-term change in dissolved inorganic nutrients in the heterotrophic Scheldt estuary (Belgium, The Netherlands). Limnol. Oceanogr. 51, 409–423.
Struyf, E., Van Damme, S., Meire, P., 2004. Possible effects of climate change on estuarine nutrient fluxes: a case study in the highly nutrified Schelde estuary (Belgium, The Netherlands). Estuarine Coastal Shelf Sci. 60, 649–661.
Struyf, E., Van Damme, S., Gribsholt, B., Middelburg, J.J., Meire, P., 2005. Biogenic silica in tidal freshwater marsh sediments and vegetation (Schelde estuary, Belgium). Mar. Ecol. Prog. Ser. 303, 51–60.
Struyf, E., Dausse, A., Van Damme, S., Bal, K., Gribsholt, B., Boschker, H.T.S., Middelburg, J.J., Meire, P., 2006. Tidal marshes and biogenic silica recycling at the land–sea interface. Limnol. Oceanogr. 51, 838–846.
Struyf, E., Smis, A., Van Damme, S., Garnier, J., Govers, G., Van Wesemael, B., Conley, D.J., Batelaan, O., Frot, E., Clymans, W., Vandevenne, F., Lancelot, C., Goos, P., Meire, P., 2010. Historical land use change has lowered terrestrial silica mobilization. Nat. Commun. 1.
Turner, R.E., Qureshi, N., Rabalais, N.N., Dortch, Q., Justic', D., Shaw, R.F., Cope, J., 1998. Fluctuating silicate:nitrate ratios and coastal plankton food webs. Proc. Natl. Acad. Sci. U. S. A. 95, 13048–13051.
Valkiers, S., Ding, T., Inkret, M., Rußе, K., Taylor, P., 2005. Silicon isotope amount ratios and molar masses for two silicon isotope reference materials: IRMM-018a and NBS28. Int. J. Mass Spectrom. 242 (2–3), 319–321. http://dx.doi.org/10.1016/j.ijms.2004.11.027.
Van Damme, S., Struyf, E., Maris, T., Ysebaert, T., Dehairs, F., Tackx, M., Heip, C., Meire, P., 2005. Spatial and temporal patterns of water quality along the estuarine salinity gradient of the Scheldt estuary (Belgium and The Netherlands): results of an integrated monitoring approach. Hydrobiologia 540, 29–45.
Vandenberghe, V., van Griensven, A., Bauwens, W., Vanrolleghem, P.A., 2005. Propagation of uncertainty in diffuse pollution into water quality predictions: application to the River Derider in Flanders, Belgium. Water Sci. Technol. 51, 347–354.
Vandervorm, P.D.J., 1980. Uptake of Si by 5 plant-species, as influenced by variations in Si-supply. Plant Soil 56, 153–156.
Vanlierde, E., De Schutter, J., Jacobs, P., Mostaert, F., 2007. Estimating and modeling the annual contribution of authigenic sediment to the total suspended sediment load in the Kleine Nete Basin, Belgium. Sediment. Geol. 202, 317–332.
Ziegler, K., Chadwick, O.A., Brzezinski, M.A., Kelly, E.F., 2005. Natural variations of delta Si-30 ratios during progressive basalt weathering, Hawaiian Islands. Geochim. Cosmochim. Acta 69, 4597–4610.